Damping of SSR Using Subsynchronous Current Suppressor With SSSC

R. Thirumalaivasan, *Member, IEEE*, M. Janaki, *Member, IEEE*, and Nagesh Prabhu, *Member, IEEE*

Abstract—Hybrid series compensation using static synchronous series compensator (SSSC) and passive series capacitor can improve the stability of the system, increases the power transfer capability and is useful for the fast control of power flow. This paper analyzes the subsynchronous resonance (SSR) characteristics of the hybrid series compensated power system in detail and proposes a simple method for the extraction of subsynchronous components of line current using filter. The extracted subsynchronous frequency component of line current is used to inject a proportional subsynchronous voltage in series with the transmission line which suppresses subsynchronous current in the transmission network. This novel technique is termed as subsynchronous current suppressor. The design of subsynchronous current suppressor is based on damping torque analysis and using genetic algorithm. A novel graphical representation of series resonance condition when SSSC is incorporated in the system is presented. The detailed study of SSR is carried out based on eigenvalue analysis, transient simulation and damping torque analysis. The results of the case study on a system adapted from IEEE First Benchmark Model demonstrates the effectiveness and robust performance of subsynchronous current suppressor in damping of SSR under various system operating conditions.

Linear analysis is performed on D-Q model of the system with SSSC and the results are tested by executing transient simulation based on detailed nonlinear three-phase model.

Index Terms—Damping torque, eigenvalue, FACTS, genetic algorithm (GA), static synchronous series compensator (SSSC), subsynchronous resonance (SSR), torsional interaction (TI), voltage source converter (VSC).

I. INTRODUCTION

SERIES compensation is an economic solution to improve the stability of transmission system and increases the power transfer capability. However, the potential inherent problem in series compensated transmission lines connected to turbo generators is subsynchronous resonance (SSR) leading to adverse torsional interactions [1]–[4] which results in shaft failure of mechanical system.

The onset of series connected FACTS controllers, like thyristor controlled series capacitor (TCSC) and static Synchronous series compensator (SSSC), has made it possible not only to regulate power flow in critical lines and also to counter the problem of SSR. SSSC has several advantages over TCSC.

SSSC is a voltage source converter (VSC) based FACTS controller, and has one degree of freedom (i.e., reactive voltage control) injects controllable reactive voltage in quadrature with the line current. The risk of SSR can be minimized by a suitable combination of hybrid series compensation consisting of passive components and VSC based FACTS controllers such as STATCOM or SSSC. The advantage of hybrid compensation is reported in [5] and shown that reactive voltage control mode of SSSC reduces the potential risk of SSR by detuning the network resonance. The SSR characteristics of TCSC and SSSC are compared in [6] and studies indicate that vernier operation of TCSC is often adequate to damp SSR whereas a subsynchronous damping controller (SSDC) with SSSC is desired for damping critical torsional modes when the line resistance is low. A method for online estimation of subsynchronous voltage components in power systems is described in [7] and used for the mitigation of SSR [8]. The damping of SSR using single phase VSC based SSSC is reported in [9].

In this paper, the analysis and simulation of a hybrid series compensated system with SSSC based on three-level 24-pulse [10] VSC is presented. The major objective is to investigate SSR characteristics of the hybrid series compensated power system in detail using both linear analysis, nonlinear transient simulation and propose a simple method for the extraction of subsynchronous component of line current using filter. The extracted subsynchronous frequency component of line current is used to inject a proportional subsynchronous voltage in series with the transmission line which suppresses subsynchronous current in the transmission network. This novel technique is termed as subsynchronous current suppressor and effectively mitigates SSR.

The study system is adapted from IEEE FBM and the analysis is executed based on damping torque analysis, eigenvalue analysis, and transient simulation. The paper is organized as follows: In Section II, modeling of SSSC and the different methods of analysis of SSR are given. Section III gives a case study and highlights the importance of filters to damp SSR under varying system parameters. Performance evaluation and the design of subsynchronous current suppressor is given in Section IV. Conclusions drawn based on case studies are given in Section V.

II. MODELING OF SSSC AND ANALYSIS OF SSR

The converter circuit of SSSC is usually a multi-pulse and/or multilevel configuration. In this work, SSSC is modeled by a combination of three-level, 24-pulse configuration with TYPE-1 controllers [11]. In three-level converter topology the magnitude of converter output voltage is controlled by varying dead angle β with fundamental switching frequency [5], [12], [13]. With the help of Type-1 controller, both the magnitude
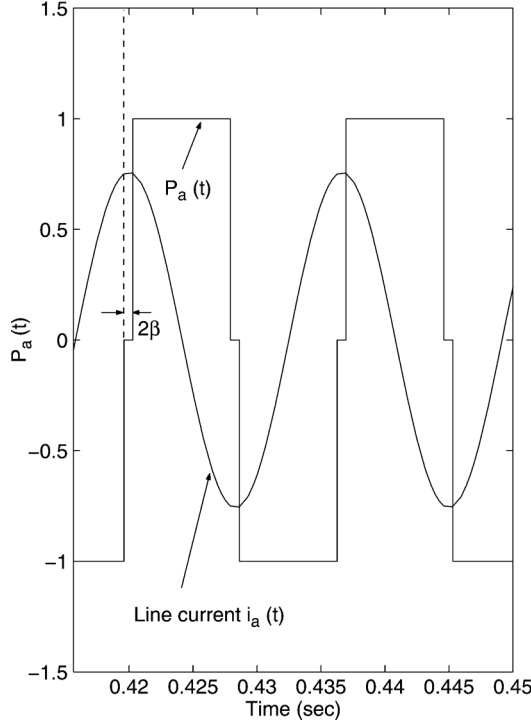
Fig. 1.   Switching function for a three-level converter.

and phase angle of converter output voltage can be controlled and the converter pole voltage is zero for the time duration of $4\beta/\omega_0$ per cycle. The harmonic distortion on the ac side is greatly reduced by using three-level converter.

In this paper, the detailed three-phase model of SSSC is developed by modelling the converter operation using switching functions. The switching function $P_a(t)$ for phase "a" is shown in Fig. 1.

The switching functions of phase b and c are similar but phase shifted successively by 120° in terms of the fundamental frequency. Assuming that the dc capacitor voltages $V_{dc1} = V_{dc2} = V_{dc}/2$, the converter terminal voltages with respect to the mid point of dc side "N" can be obtained as

$$\begin{bmatrix} V_{aN}^i \\ V_{bN}^i \\ V_{cN}^i \end{bmatrix} = \begin{bmatrix} P_a(t) \\ P_b(t) \\ P_c(t) \end{bmatrix} \frac{V_{dc}}{2} \qquad (1)$$

and the converter output voltages with respect to the neutral of transformer can be expressed as

$$\begin{bmatrix} V_{an}^i \\ V_{bn}^i \\ V_{cn}^i \end{bmatrix} = \begin{bmatrix} S_a(t) \\ S_b(t) \\ S_c(t) \end{bmatrix} V_{dc} \qquad (2)$$

where $S_a(t) = (P_a(t)/2) - [P_a(t) + P_b(t) + P_c(t)/6] S_a(t)$ is the switching function for phase "a" of a six-pulse three-level VSC. Similarly for phase "b", $S_b(t)$ and for phase "c", $S_c(t)$ can be derived. The peak value of the fundamental and harmonics in the phase voltage V_{an}^i are found by applying Fourier analysis on the phase voltage and can be expressed as

$$V_{an(h)}^i = \frac{2}{h\pi} V_{dc} cos(h\beta) \qquad (3)$$

where $h = 1, 5, 7, 11, 13$ and β is the dead angle (period) during which the converter pole output voltage is zero. We can eliminate the 5th and 7th harmonics by using a twelve-pulse VSC, which combines the output of two six-pulse converters using transformers.

The switching functions for first twelve-pulse converter are given by

$$S_{1a}^{12}(t) = S_{1a}(t) + \frac{1}{\sqrt{3}} \left(S_{1a}'(t) - S_{1c}'(t) \right),$$

$$S_{1b}^{12}(t) = S_{1b}(t) + \frac{1}{\sqrt{3}} \left(S_{1b}'(t) - S_{1a}'(t) \right),$$

$$S_{1c}^{12}(t) = S_{1c}(t) + \frac{1}{\sqrt{3}} \left(S_{1c}'(t) - S_{1b}'(t) \right)$$

where

$$S_{1x}'(t) = S_{1x}\left[t + \frac{2\pi}{\omega_o} \frac{1}{12} \right]$$

$$S_{1x}(t) = S_x\left[t + \frac{\pi}{\omega_o} \frac{1}{24} \right], \quad x = a, b \ and \ c. \qquad (4)$$

The switching functions for second twelve-pulse converter are given by

$$S_{2a}^{12}(t) = S_{2a}(t) + \frac{1}{\sqrt{3}} \left(S_{2a}'(t) - S_{2c}'(t) \right),$$

$$S_{2b}^{12}(t) = S_{2b}(t) + \frac{1}{\sqrt{3}} \left(S_{2b}'(t) - S_{2a}'(t) \right),$$

$$S_{2c}^{12}(t) = S_{2c}(t) + \frac{1}{\sqrt{3}} \left(S_{2c}'(t) - S_{2b}'(t) \right)$$

where

$$S_{2x}'(t) = S_{2x}\left[t + \frac{2\pi}{\omega_o} \frac{1}{12} \right]$$

$$S_{2x}(t) = S_x\left[t - \frac{\pi}{\omega_o} \frac{1}{24} \right], \quad x = a, b \ and \ c. \qquad (5)$$

The switching functions for a 24-pulse converter are given by

$$S_x^{24}(t) = S_{1x}^{12}(t) + S_{2x}^{12}(t), \quad x = a, b \ and \ c. \qquad (6)$$

The two 12-pulse converters are interfaced to obtain three-level 24-pulse VSC based SSSC. The converter output voltage are given by

$$V_{xn}^i = S_x^{24}(t) * V_{dc} \qquad (7)$$

where $x = a, b, c$.

If the switching functions are approximated by their fundamental components (neglecting harmonics) for a 24-pulse three-level converter, we get

$$V_{an}^i = \frac{8}{\pi} V_{dc} cos(\beta) sin(\omega_o t + \phi + \gamma) \qquad (8)$$

and V_{bn}^i, V_{cn}^i are phase shifted successively by 120°.

The line current is given by $i_a = \sqrt{(2/3)} I_a sin(\omega_o t + \phi)$ and i_b, i_c are phase shifted successively by 120°. Note that γ is the angle by which the fundamental component of converter output voltage leads the line current. It should be noted that γ is nearly equal to $\pm(\pi/2)$ depending upon whether SSSC injects
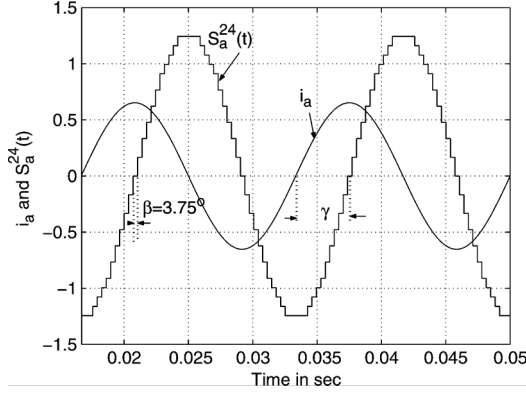
Fig. 2. Switching function of 24-pulse three-level converter analogous to a 48-pulse converter when $\beta = 3.75°$.
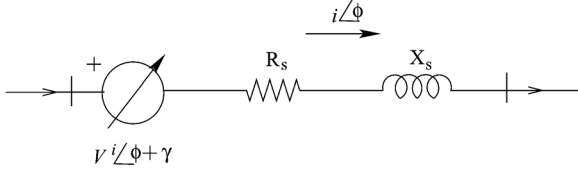

Fig. 3. Schematic representation of SSSC.

inductive or capacitive voltage. Neglecting converter losses we can get the expression for dc capacitor current as

$$[i_{dc}] = - \begin{bmatrix} S_a^{24}(t) & S_b^{24}(t) & S_c^{24}(t) \end{bmatrix} \begin{bmatrix} i_a \\ i_b \\ i_c \end{bmatrix}. \tag{9}$$

A particular harmonic reaches zero, when $2\beta = 180°/h$. At $\beta_{optimum} = 3.75°$, the switching function for phase "a" is shown in Fig. 2 and indicates that 24-pulse three-level converter behaves like a 48-pulse converter when $\beta = 3.75°$ as 23rd and 25th harmonics are negligibly small.

A. Mathematical Model of SSSC in D-Q Frame of Reference

When switching functions are approximated by their fundamental frequency components, neglecting harmonics, SSSC can be modeled by transforming the three-phase voltages and currents to D-Q variables using Kron's transformation [15]. The SSSC can be represented functionally as shown in Fig. 3.

In Fig. 3, R_s and X_s are the resistance and reactance of the interfacing transformer of VSC. The magnitude control of converter output voltage V^i is achieved by modulating the conduction period affected by dead angle β of a converter while the dc voltage is maintained constant.

The converter output voltage can be represented in the D-Q frame of reference as

$$V^i = \sqrt{V_D^{i\,2} + V_Q^{i\,2}} \tag{10}$$

where V_D^i and V_Q^i are the D and Q components of SSSC injected voltage V^i and are defined as follows:

$$V_D^i = K_m V_{dc} sin(\phi + \gamma) \tag{11}$$
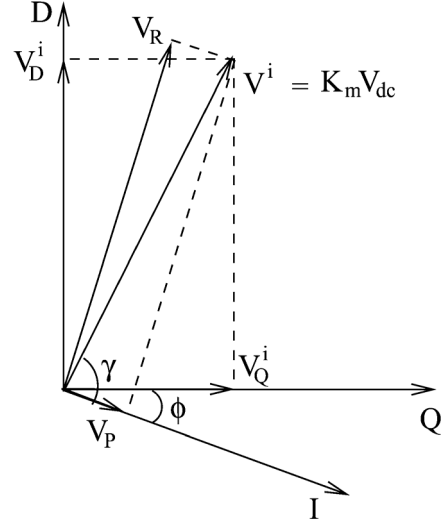$$V_Q^i = K_m V_{dc} cos(\phi + \gamma) \tag{12}$$

Fig. 4. Phasor diagram of SSSC.

where k_m is the modulation index [5]. For a 24-pulse three-level converter the modulation index is a function of dead angle β and is given by $k_m = k\rho cos\beta$. ρ is the transformation ratio of SSSC interfacing transformer. From the control point of view it is convenient to define the real voltage V_P and reactive voltage V_R which are the components of V^i in phase and quadrature with line current I, respectively, and the phasor diagram is shown in Fig. 4. V_P and V_R in terms of variables in D-Q frame (V_D^i and V_Q^i) are obtained as

$$V_R = V_D^i \cos \phi - V_Q^i \sin \phi \tag{13}$$
$$V_P = V_D^i \sin \phi + V_Q^i \cos \phi. \tag{14}$$

Here, positive V_R indicates inductive mode of operation of SSSC and positive V_P indicates that SSSC absorbs active power from the line.

The dc side capacitor is described by the dynamical equation as

$$\frac{dV_{dc}}{dt} = -\frac{\omega_b}{b_c}I_{dc} - \frac{\omega_b g_c}{b_c}V_{dc} \tag{15}$$

where $I_{dc} = -[k_m sin(\phi + \gamma)I_D + k_m cos(\phi + \gamma)I_Q]$, $\omega_b = 2\pi f_b$, (f_b—base frequency), b_c—susceptance of dc side capacitor, g_c—conductance which accounts for losses.

I_D and I_Q are the D-Q components of the line current I. ϕ is the phase angle of line current and γ is the angle by which converter output voltage leads the line current.

B. SSSC Voltage Control (Three-Level VSC)

In Type-1 controller both magnitude (modulation index k_m) and phase angle of converter output voltage (γ) are controlled. The dc side capacitor voltage is maintained at a constant voltage by controlling real voltage V_P. The real voltage reference $V_{P(ord)}$ is obtained as the output of dc voltage controller.

The reactive voltage reference $V_{R(ord)}$ may be kept constant or obtained from a power scheduling controller. However, for the SSR analysis constant reactive voltage control is considered.
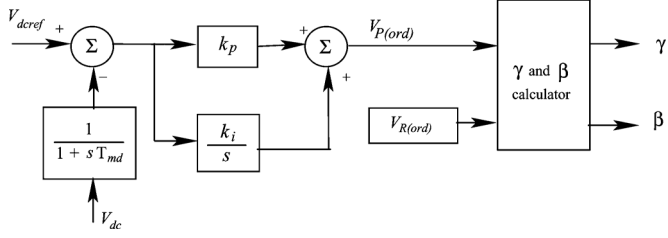
Fig. 5. Type-1 controller for SSSC.

Fig. 6. Modified IEEE First Benchmark Model with SSSC.

It should be noted that harmonic content of the SSSC injected voltage would vary depending upon the operating point since magnitude control will also govern the switching.

The dc capacitor voltage reference can be varied (depending on reactive voltage reference) so as to give optimum harmonic performance. In three-level 24-pulse converter, dc voltage reference may be adjusted by a slow controller to get optimum harmonic performance at $\beta_{optimum} = 3.75°$ in steady state.

The structure of type-1 controller for SSSC is given in Fig. 5. In this figure, γ and β are calculated as

$$\gamma = tan^{-1}\left[\frac{V_{R(ord)}}{V_{P(ord)}}\right] \tag{16}$$

$$\beta = cos^{-1}\left[\sqrt{\frac{V_{P(ord)}^2 + V_{R(ord)}^2}{k\rho V_{dc}}}\right]. \tag{17}$$

C. Analysis of Subsynchronous Resonance

The SSR is analyzed based on damping torque, eigenvalue analysis and transient simulation [14]. The steady-state SSR is analyzed based on damping torque and eigenvalue analysis with linearized models at the operating point. The transient SSR is analyzed by transient simulation with nonlinear model of the system, where the generator stator transients are taken into account with the detailed generator model (2.2) [15]. The transmission line is modeled by lumped resistance and inductance to consider the effect of line transients.

The graphical representation of resonance condition using impedance function of SSSC on single phase basis is presented in this paper in Section III and is a novel representation to validate the results of damping torque and eigenvalue analysis. It shows the variation of inductive and capacitive reactances with frequency varied from 10–300 rad/s. This graphical representation presents a clear picture of possible SSR condition in the system.

III. CASE STUDY

The system under study is adapted from IEEE FBM [16] which consists of a turbine, generator (2.2 model), series compensated long transmission line and SSSC injecting a series voltage in the transmission line is shown in Fig. 6.

The analysis is carried out by considering the following assumptions and initial operating condition.
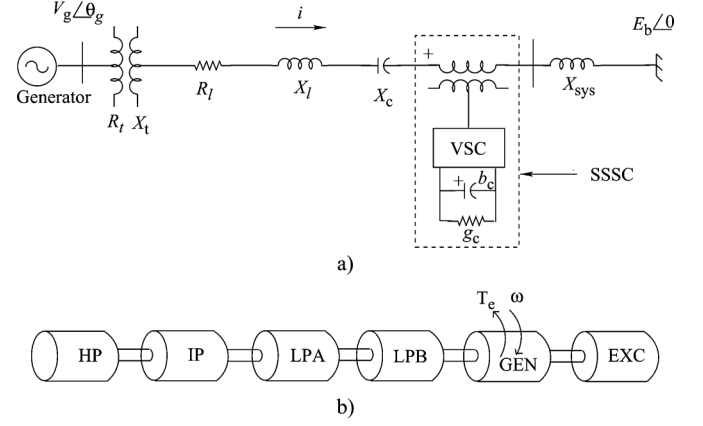
1) The generator supplies power (P_g) of 0.9 p.u. to the transmission line.
2) The mechanical input power to the turbine is made constant.
3) The total series compensation is kept at 0.76 p.u. The study is carried out for the following cases
   Case-1:Without SSSC Case-2:With SSSC In Case-1, Fixed capacitor alone is used for the series compensation with $X_C = X_{C1} = 0.76$ p.u. and in Case-2, hybrid compensation is used wherein 0.25 p.u. of series compensation is met by SSSC $(X_{SSSC} = V_R/I)$ and the remaining compensation is provided by fixed capacitor $X_C = X_{C2} = 0.51$ p.u.
4) In transient simulation, a small mechanical disturbance of 10% step decrease in mechanical input torque is applied at 0.5 s and restored at 1 s1 s is considered. To validate the effectiveness of SSSC under severe fault, a three-phase to ground fault applied at generator terminal at 1 s and cleared after three cycles is considered.

A. Eigenvalue Analysis

The eigenvalues of the system matrix for the linearized system about an operating point are given in Table I for case 1 and case 2. It should be noted that, without SSSC, i.e., in case-1, mode-1 becomes unstable at the operating point considered. It is to be noted that with the inclusion of SSSC, (case-2) undamping of mode-1 is reduced and the frequency of network mode (sub) is increased to 128.4 rad/s. This network mode closely matches with torsional mode-2 and it turns out to be unstable. This indicates that the introduction of SSSC for series compensation increases and shifts the network resonant frequency.

B. Transient Simulation

The transient simulation is carried out for the combined nonlinear system which includes SSSC represented by both D-Q and three-phase model using MATLAB-SIMULINK [17].

The transient simulation results for a step change of 10% decrease in the mechanical input torque applied at 0.5 s and restored at 1 s with three-phase model of three-level VSC based

TABLE I
EIGENVALUES OF THE COMBINED SYSTEM WITH AND WITHOUT SSSC

Torsional Mode	$Case - 1 : Without\ SSSC$ $(X_{c1} = 0.76\ p.u)$	$Case - 2 : With\ SSSC$ $(X_{c2} = 0.51\ p.u$ $and\ X_{SSSC} = 0.25\ p.u)$
0	$-2.6346 \pm j\ 9.3403$	$-1.7105 \pm j\ 8.2100$
1	$2.8086 \pm j\ 97.473$	$0.0977 \pm j\ 99.080$
2	$-0.0807 \pm j\ 126.960$	$0.1578 \pm j\ 127.000$
3	$-0.6582 \pm j\ 160.490$	$-0.6670 \pm j\ 160.460$
4	$-0.3740 \pm j\ 202.850$	$-0.3790 \pm j\ 202.850$
5	$-1.8504 \pm j\ 298.170$	$-1.8504 \pm j\ 298.170$
Network mode (sub)	$-4.9272 \pm j\ 99.378$	$-3.7700 \pm j\ 128.410$
Network mode (super)	$-5.7326 \pm j\ 658.090$	$-4.8842 \pm j\ 590.200$

Fig. 8. Variation of damping torque with and without SSSC.
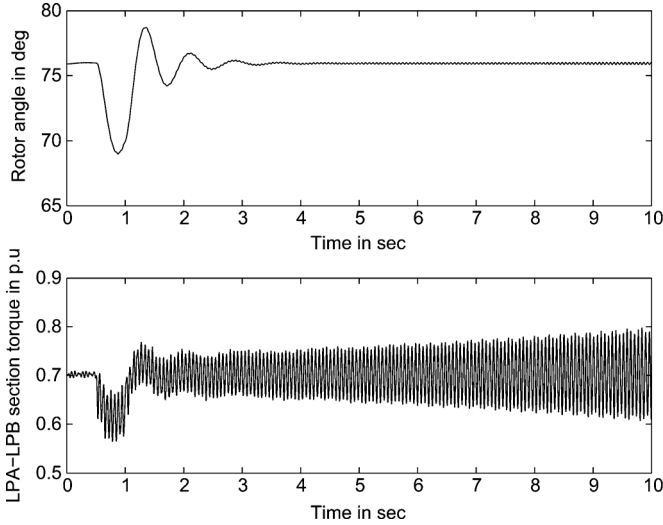

Fig. 7. Variation of rotor angle and LPA-LPB section torque for step change in input mechanical torque with three-phase model of three-level VSC based SSSC.

SSSC is shown in Fig. 7. It is clear from Fig. 7 that the system is unstable as the LPA-LPB section torque grows with time.

C. Discussion

The SSR problems under various operating conditions can be predicted by using damping torque analysis. The correlation of damping torque analysis and eigenvalue results in predicting torsional mode stability is discussed in detail in [18] which demonstrates the importance of damping torque analysis to determine the torsional mode stability.

1) Damping Torque Analysis With Linearized Model of SSSC: Variation of damping torque is shown in Fig. 8 for case 1 and 2. It is to be noted that without SSSC (case-1), damping torque goes maximum negative at a frequency of about 98 rad/s and matches with torsional mode-1 frequency and severe torsional interactions are expected. In case-2 with the inclusion
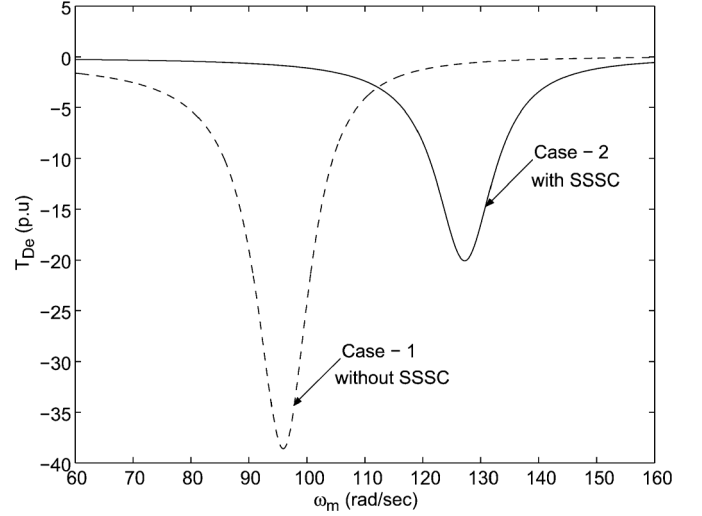
of SSSC, the peak negative damping is significantly reduced and shifts the network mode frequency (subsynchronous) and hence undamping of torsional mode-1 is also reduced. The shifted subsynchronous electrical frequency matches with mode-2 torsional frequency (127 rad/s) and the corresponding torsional mode becomes unstable. These results are consistent with eigenvalue analysis.

2) Graphical Representation of Resonance Condition: The representation of impedance function of SSSC in single phase basis $(Z_{se(1ph)}(j\omega))$ from that of D-Q axis $[Z_s]$ is given below. To obtain $[Z_s]$, the SSSC equations (along with controller) are linearized at the operating point and expressed as

$$[\Delta\dot{X}_s] = [A_s][\Delta X_s] + [B_s]\begin{bmatrix}\Delta i_D \\ \Delta i_Q\end{bmatrix} \tag{18}$$

$$\begin{bmatrix}\Delta v_D^i \\ \Delta v_Q^i\end{bmatrix} = [C_s][\Delta X_s] + [D_s]\begin{bmatrix}\Delta i_D \\ \Delta i_Q\end{bmatrix} \tag{19}$$

$$\begin{bmatrix}\Delta v_D^i \\ \Delta v_Q^i\end{bmatrix} = [Z_s]\begin{bmatrix}\Delta i_D \\ \Delta i_Q\end{bmatrix} \tag{20}$$

where

$$[Z_s] = \begin{bmatrix}Z_{sDD} & Z_{sDQ} \\ Z_{sQD} & Z_{seQQ}\end{bmatrix} = [C_s][s[I] - A_s]^{-1}[B_s] + [D_s]$$

$[I]$ is identity matrix.

$$Z_{se(1ph)}(j\omega) = R_{se} + jX_{se}$$
$$= \frac{1}{2}\left[\{Z_{sDD}(j(\omega - \omega_0)) + Z_{sQQ}(j(\omega - \omega_0))\}\right.$$
$$+ j\{Z_{sDQ}(j(\omega - \omega_0))$$
$$\left. - Z_{sQD}(j(\omega - \omega_0))\}\right]. \tag{21}$$

The resistance R_{se} and the emulated reactance X_{se} of SSSC on single phase basis as a function of frequency ω_{er} is computed for case-2 with $X_{sssc} = 0.25$ p.u. It is found that, the resistance
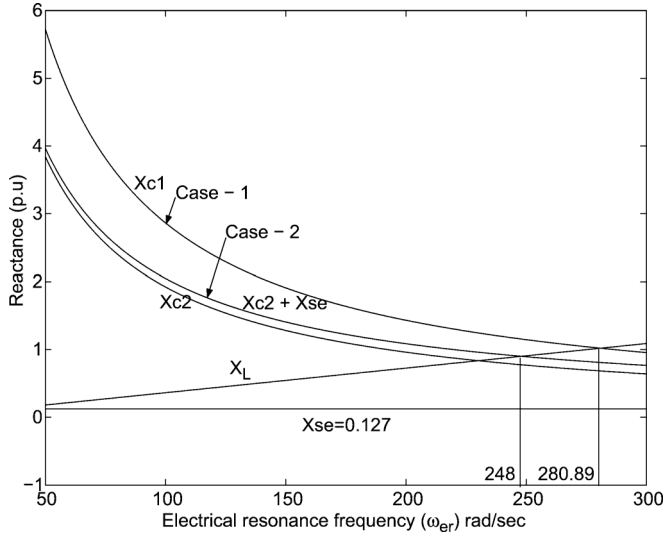
Fig. 9. Graphical representation of resonance conditions with and without SSSC.

is negligible while the emulated reactance $X_{se} = 0.127$ p.u is practically constant with frequency as shown in Fig. 9.

The graphical representation of resonance frequency is shown in Fig. 9 for cases 1 and 2. It shows the variation of inductive and capacitive reactances with frequency varied from 10–300 rad/s. In case-1, when the fixed capacitor provides 76% of compensation ($X_{c1} = 0.76$ p.u.) the resonance occurs at $\omega_{er} = 280.89$ rad/s, where $X_{c1} = X_L$. In case-2, where compensation of 76% is met by $X_{c2} = 51\%$ and $X_{SSSC} = 25\%$, the effective capacitive reactance ($X_{c2} + X_{se}$) is obtained by adding the constant reactance X_{se} offered by SSSC to that offered by fixed capacitor X_{c2}. The variation of effective capacitive reactance ($X_{c2} + X_{se}$) with frequency is also shown in Fig. 9. Now the resonance occurs at a frequency of $\omega_{er} = 248$ rad/s, where ($X_{c2} + X_{se}) = X_L$ and this is consistent with the subsynchronous network mode frequency ($\omega_m = \omega_0 - \omega_{er} = 377 - 248 = 129$ rad/s) as obtained by eigenvalue analysis and about 127 rad/s obtained by damping torque analysis with SSSC.

The effect of additional series compensation by SSSC to supplement the existing fixed capacitor X_{c2} is to increase the electrical resonance frequency of the network. However, this increase in frequency is not significant as compared to that obtained with the equivalent fixed capacitor offering additional compensation (case-1, $\omega_{er} = 280.89$ rad/s in this case). This illustrates that the SSSC is not strictly SSR neutral however, it offers a reactance which remain practically constant with frequency.

Hence it is obvious that, to mitigate SSR, the damping of critical torsional modes should be improved by reducing the negative damping. This paper investigates the application of subsynchronous current suppressor for damping SSR. The subsynchronous components of line current can be extracted from the network using filters with narrow pass band. The extracted subsynchronous line current components are used to inject proportional voltages by SSSC to suppress the subsynchronous currents flowing in the generator. A systematic method to extract

subsynchronous frequency components using filters and mitigation of SSR using subsynchronous current suppressor is presented in the following section.

IV. DESIGN OF SUBSYNCHRONOUS CURRENT SUPPRESSOR

Damping of SSR can be obtained by designing a subsynchronous damping controller (SSDC) which provides positive damping in the range of critical torsional mode of frequencies [14]. Damping of SSR using STATCOM is achieved by SSDC which takes Thevenin voltage signal (a synthesized voltage) [19] using locally available STATCOM bus voltage and is used to modulate the reactive reference current to improve the damping of unstable torsional modes. The present work proposes the improvement of damping of critical torsional modes by extracting subsynchronous components of line current and injecting a proportional voltage to suppress the subsynchronous frequency currents. This is a simple method which reduces the magnitude of subsynchronous currents flowing through the generator and is termed as subsynchronous current suppressor (SSCS).

The extraction of subsynchronous frequency current component is achieved by band-pass filters operate in rotating D-Q coordinates. Accordingly the tuning of filters depends on the multimass turbine-generator shaft torsional frequencies. Hence it is adequate to design filter based on the knowledge of torsional mode frequencies to extract the subsynchronous frequency components to damp SSR. In this paper, the IEEE FBM with six mass mechanical system is considered, which has five natural torsional mode frequencies [4]. The torsional mode frequency is taken as the center frequency and the pass band of filter is chosen from the eigen value analysis in which torsional mode is unstable for the band of subsynchronous network mode frequencies closer to that of critical torsional frequency. The frequency response of band-pass filters for all critical torsional modes are shown in Fig. 10. This method of filter design is also valid for any transmission network topologies as only the complement of network resonance frequencies ($\omega_0 - \omega_{er}$) matches with torsional frequencies (ω_m) cause SSR. The block diagram of subsynchronous current suppressor to extract subsynchronous frequency components from the line current is shown in Fig. 11. Two band-pass filters (in D-Q frame) are used to extract each torsional frequency component I_{Dsub} and I_{Qsub} from the line current I_D and I_Q. Each filter set is effective only for their corresponding torsional mode frequency and improve the damping of respective torsional modes by reducing the negative damping. Subsynchronous current suppressor extracts subsynchronous frequency currents corresponding to modes 1, 2, 3, and 4 passed through appropriate gains k_1 to k_8 for obtaining V_{Dsub} and V_{Qsub} and sum up the signal to obtain V_{Ds} and V_{Qs} as mentioned in the following:

$$V_{Ds} = \sum_m V_{Dsub}$$

$$V_{Qs} = \sum_m V_{Qsub}$$

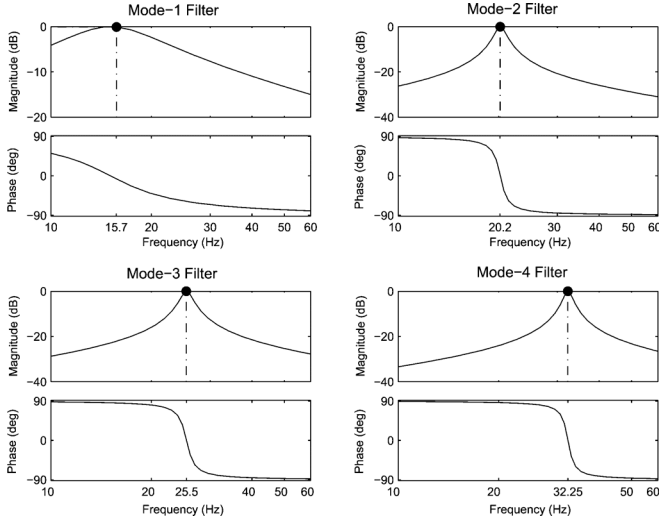where m is the torsional mode (m = 1, 2, 3, and 4).

Fig. 10.   Frequency response of band-pass filters.
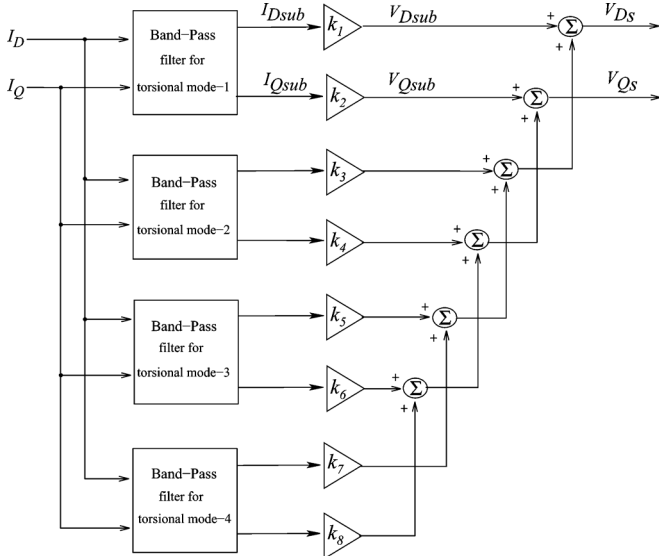

Fig. 11.   Block diagram of subsynchronous current suppressor.

Since modal inertia of torsional mode 5 is very high, mode 5 is never excited and filter to extract mode 5 frequency component is not desired. The extracted subsynchronous voltage orders V_{Ds} and V_{Qs} (in D-Q frame of reference) are transformed to inphase and quadrature components $V_{P(sub)}$ and $V_{R(sub)}$, respectively, and are used to modulate the in phase and quadrature voltage orders $V_{P(ord)}$ and $V_{R(ord)}$ of SSSC as shown in Fig. 12.

The subsynchronous frequency components of various modes extracted from line current are passed through a suitable gains k_1 to k_8 and the damping of critical torsional modes are improved by properly tuning k_1 to k_8 using GA making use of damping torque analysis. Genetic algorithm has been used to optimize the parameters of control system that are complex and difficult to solve by conventional optimization methods [20]. In the following section optimization of subsynchronous current suppressor parameters based on damping torque using GA is presented.
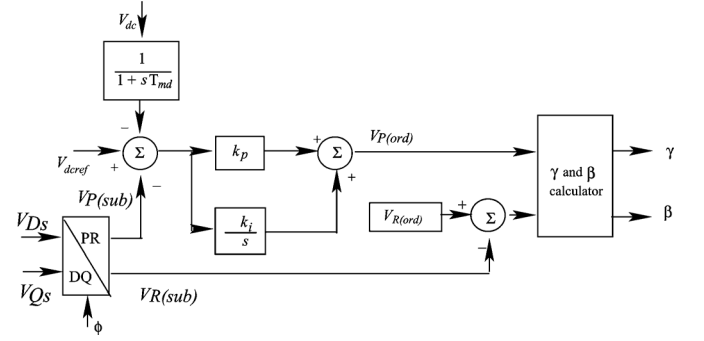

Fig. 12.   Type-1 controller for SSSC with extracted subsynchronous frequency components from subsynchronous current suppressor.

A. Application of Genetic Algorithm for Optimization of Subsynchronous Current Suppressor Parameters

The objective of subsynchronous current suppressor is to enhance the damping torque by reducing the negative damping at critical torsional mode frequencies. The synchronizing torque at torsional frequencies are not significantly affected by the electrical network (with or without damping controller [14]), hence it is simpler to design subsynchronous current suppressor by optimizing the gains k_1 to k_8 with the objective to minimize the deviations between the desired damping torque$[T_{De(des)}]$ and actual damping torque (T_{De}) to reduce the negative damping in the range of all torsional mode frequencies. Genetic algorithm is adopted for optimizing the gains of subsynchronous current suppressor to ensure the stability in the complete range of all critical torsional mode frequencies.

On the basis of these facts, the objective function is defined as

$$\text{minimize } E = \sum_{X_c} \sum_{\omega} \left[T_{De(des)} - T_{De}(\omega) \right]^2 \qquad (22)$$

where $T_{De}(\omega) = \Re[\Delta T_e(j\omega)/\Delta S_m(j\omega)]$, ΔS_m is the p.u. deviation in generator rotor speed and ΔT_e is the p.u. change in electric torque, E is the summation of squared error over the range of series compensation ($X_c = 0.05$ to 0.75 p.u and $X_{sssc} = 0.25$ p.u., and $50 \leq \omega \leq 300$ rad/s) up to 100%. To ensure the stability of the system, the objective function is subjected to the constraint that

$$\text{Real part of all eigenvalues} < 0. \qquad (23)$$

In order that subsynchronous current suppressor minimizes the negative damping, the desired damping torque is taken as positive while ensuring all eigenvalues to have negative real parts. However, it was noticed that, when the value of $T_{De(des)}$ is large positive, network mode becomes unstable. Here, the desired damping torque $T_{De(des)}$ is taken as 8 p.u. for the entire range of torsional frequencies. The outcome of GA optimization is the gains k_1 to k_8 which remain unchanged at various operating conditions while ensuring system stability.

B. Analysis of SSR With Subsynchronous Current Suppressor

The analysis is performed based on eigenvalue analysis, damping torque analysis and transient simulation. D-Q model of SSSC is considered for damping torque and eigenvalue
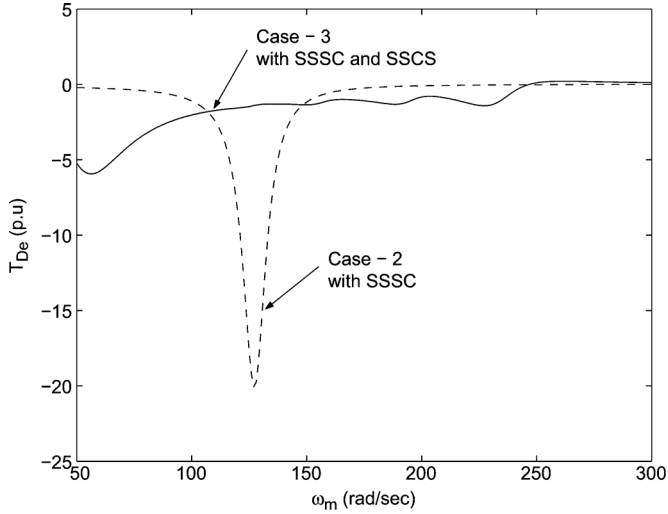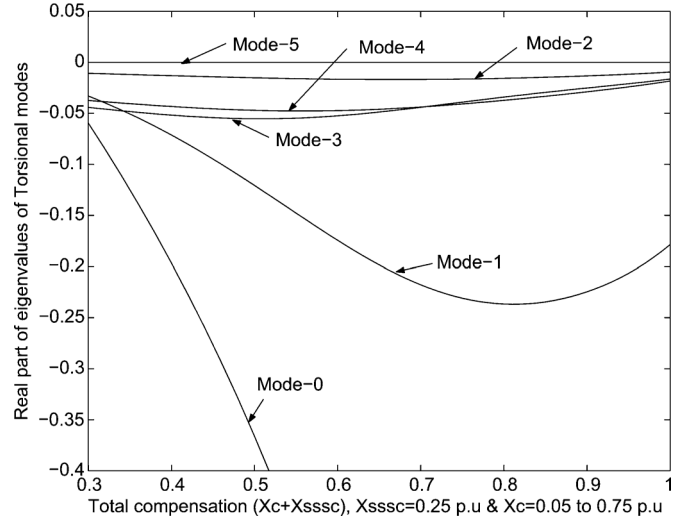
Fig. 13. Damping torque with SSSC and SSCS.

Fig. 14. Variation of real part of eigenvalue of torsional modes with compensation level with SSSC and SSCS.

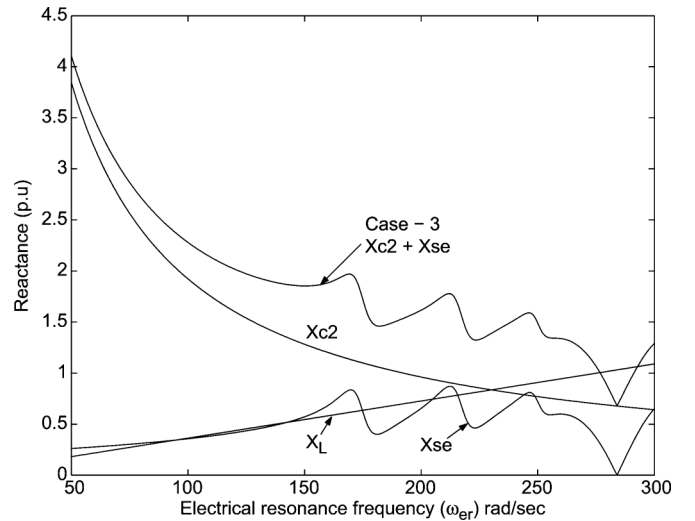Fig. 15. Variation of emulated reactance of SSSC with SSCS.

analysis and the detailed three-phase model of SSSC is used for transient simulation.

1) Damping Torque Analysis: The damping torque with SSSC and GA optimized subsynchronous current suppressor (case-3) is shown in Fig. 13. It is to be noted that, the peak negative damping is greatly reduced with subsynchronous current suppressor.

The negative damping is negligible in the range of torsional frequencies (60–300 rad/s) and the system is expected to be stable with the intrinsic mechanical damping and the transmission line resistance. The variation of real part of eigenvalue of all torsional modes with compensation level is shown in Fig. 14 when the mechanical damping is neglected. Referring to Fig. 14, it is observed that all the torsional modes are stable with the proposed subsynchronous current suppressor using optimal parameters when the hybrid compensation is varied from 0.3 p.u. to 1 p.u. This demonstrates the robustness of the designed subsynchronous current suppressor in damping subsynchronous oscillations in the range of series compensation.

The variation of total effective capacitive reactance incorporating subsynchronous current suppressor $(X_{C2} + X_{se})$ is shown in Fig. 15 (case-3), it is observed that X_{se} is not constant with frequency due to the presence of filters used in subsynchronous current suppressor. The total effective capacitive reactance incorporating subsynchronous current suppressor $(X_{C2} + X_{se})$ never becomes equal to X_L in the frequency range of 50–275 rad/s. It is to be noted that between 275 to 300 rad/s, the effective capacitive reactance is equal to X_L at two frequencies, which are close to torsional mode-5. Since the modal inertia of mode-5 is high, it is unaffected and remain stable as shown in Fig. 14. All other torsional modes (1–4) and swing mode (0) are also found to be stable when hybrid compensation is varied from 0.3 p.u. to 1 p.u. This clearly indicates that the designed subsynchronous current suppressor ensures that the series compensated power system is free from SSR.

2) Eigenvalue Analysis: The eigenvalues of the system with three-level VSC-based SSSC and SSCS are shown in Table II.

Comparing the eigenvalue results of with SSSC and without subsynchronous current suppressor (Table I, col-2) and with the

presence of both SSSC and subsynchronous current suppressor (Table II), the following observations can be made.

1) With subsynchronous current suppressor, the damping of torsional modes 1 and 2 has significantly improved.

TABLE II
EIGENVALUES OF THE COMBINED SYSTEM WITH SSSC AND SSCS

Torsional mode	$Case-3: With\ SSSC\ and\ SSCS$ $(X_{c2} = 0.51\ p.u\ and\ X_{SSSC} = 0.25\ p.u)$
0	$-1.1747 \pm j\ 8.3318$
1	$-0.4540 \pm j\ 98.468$
2	$-0.0887 \pm j\ 126.990$
3	$-0.6842 \pm j\ 160.530$
4	$-0.3992 \pm j\ 202.890$
5	$-1.8504 \pm j\ 298.170$
Network mode subsynchronous $-14.288 \pm j\ 233.390$	
Network mode supersynchronous $-3.7098 \pm j\ 616.580$	

2) The damping of torsional mode-3 and mode-4 is marginally increased with subsynchronous current suppressor.
3) Damping of mode-0 is marginally decreased.
4) Modal inertia of Mode-5 is very high and hence is not excited.
5) The damping of subsynchronous network mode is significantly increased with subsynchronous current suppressor.

3) Transient Simulation: The transient simulation has been carried out for the overall system including SSSC with subsynchronous current suppressor using MATLAB-SIMULINK [17]. Fig. 16 shows the simulation results for full load of $P_g = 0.9$ p.u. with the step change of 10% decrease in the input mechanical torque applied at 0.5 s and removed at 1 s and subsynchronous current suppressor is activated at $t = 5$ s. It is observed that the section torque is growing with time until $t = 5$ s, when subsynchronous current suppressor is activated at $t = 5$ s, the oscillations of shaft section torque decays with time. The FFT analysis of the LPA-LPB section torque is performed between 3–8 s with the time spread of 1 s and is shown in Fig. 17. Referring to Fig. 17, it is observed that in the time span of 3–5 s, the mode-1 component is predominant and increases with time. When SSCS is activated at 5 s, the mode-1 component decays with time and demonstrates the effectiveness of subsynchronous current suppressor to suppress the subsynchronous frequency components in the line. Transient simulation for three-phase fault at generator terminal with fault impedance as given in IEEE FBM [16] is applied at 1 s cleared after three cycles with $P_g = 0.9$ p.u. and $P_g = 0$ p.u. are shown in Figs. 18 and 19, respectively. The SSCS gain values k_1 to k_8 remain unchanged in all operating points and is observed that with SSCS the oscillations of section torque decay with time. The line current and D-Q components of subsynchronous current when $P_g = 0$ p.u and following three-phase fault at generator terminals with SSCS are shown in Fig. 20. It shows that SSCS extracts subsynchronous frequency components even when the fundamental frequency line current is zero ($P_g = 0$ p.u). It is to be noted that, under disturbance conditions the line is expected to carry currents due to energy exchange between mechanical and electrical system at their natural frequencies. As a result, the transmission line carries both subsynchronous and supersynchronous frequency current components ($\omega_0 \pm \omega_m$). The supersynchronous frequency currents in the network contributes positive damping torque [4]. It is the subsynchronous frequency component of network currents that cause negative damping. Under disturbances, torsional mode-1 (98 rad/s) gets excited for the operating points considered which is most severe torsional mode and contributes maximum negative damping. The FFT analysis of phase "a" line current is performed in the time span of 1–1.4 s and 2–4 s as shown in Fig. 21 and it is interesting to note that the subsynchronous network frequency (ω_{er}) components of line current decreases with time. From the result of FFT analysis of phase "a" of line current, it is evident that the SSCS is effective in extracting and suppressing the subsynchronous frequency components of line current even when the fundamental frequency line current is zero. This clearly demonstrates the effectiveness and robust performance of the proposed SSCS in mitigating SSR while k_1 to k_8 gain values remain unchanged under varying operating conditions.
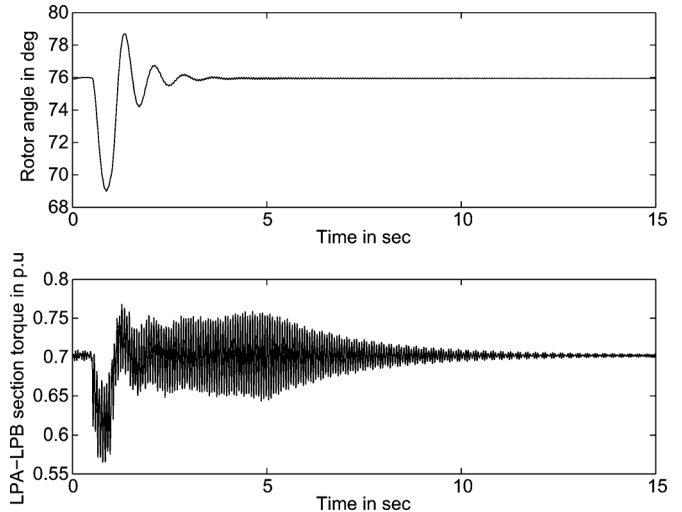

Fig. 16. Variation of rotor angle oscillation and LPA-LPB section torque for step change in mechanical input torque with SSSC and subsynchronous current suppressor is activated at $t = 5$ s.
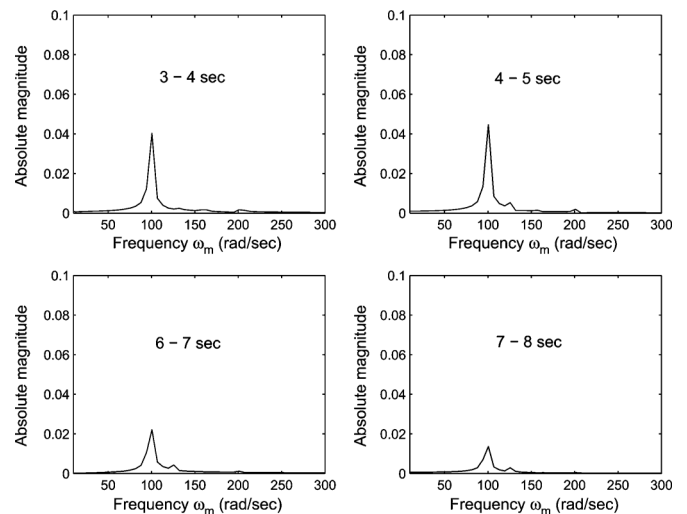

Fig. 17. FFT analysis of LPA-LPB section torque for case-3 ($X_c = 0.51$ p.u. and $X_{SSSC} = 0.25$ p.u., SSCS activated at 5 s).

C. Discussion

We propose a novel method to extract the subsynchronous frequency components from the line current using filters. The design of subsynchronous current suppressor is based on the damping torque method [18], and genetic algorithm is adopted for optimizing subsynchronous current suppressor filter gains. The results demonstrate the robust performance of the system in the entire compensation level and for the different operating conditions.

In the present work, hybrid compensation is used. While the series active compensation is provided by the VSC based SSSC for the enhancement of power transfer capability, the use of subsynchronous current suppressor mitigates the SSR. The damping of all torsional modes in the entire range of compensation level is improved without the risk of SSR by employing subsynchronous current suppressor.
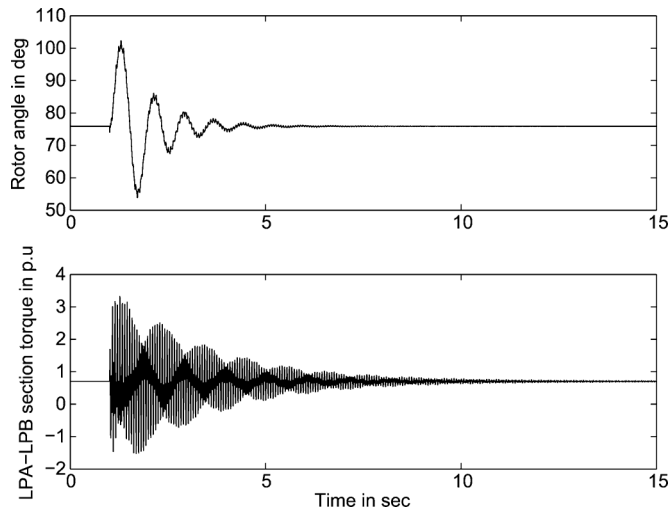
Fig. 18. Variation of rotor angle and LPA-LPB section torque for three-phase fault at generator terminal with SSSC and subsynchronous current suppressor when $P_g = 0.9$ p.u.
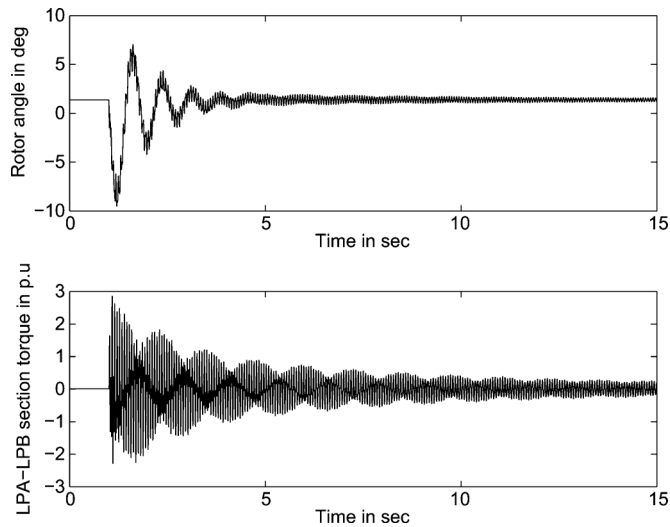

Fig. 19. Variation of rotor angle and LPA-LPB section torque for three-phase fault at generator terminal with SSSC and subsynchronous current suppressor when $P_g = 0$ p.u.
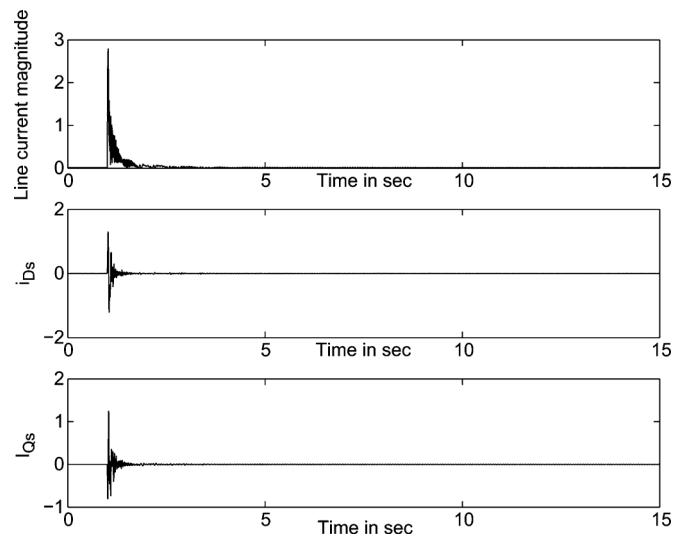

Fig. 20. Line current magnitude and D-Q components of subsynchronous current for three-phase fault at generator terminal when $P_g = 0$ p.u.

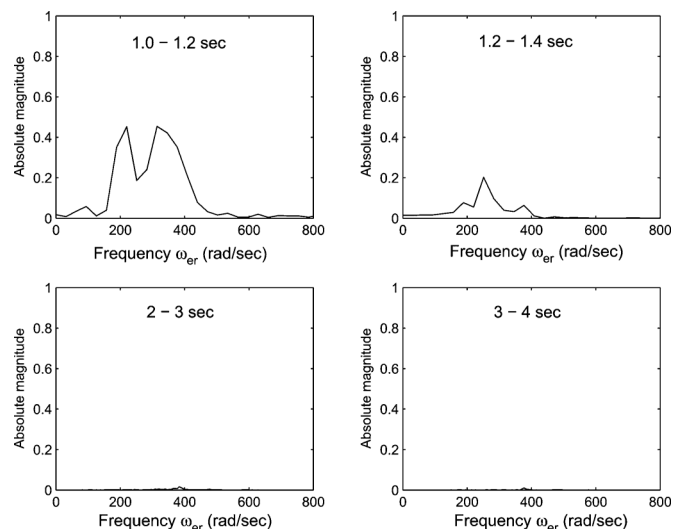Fig. 21. FFT analysis of line current in phase "a" when $P_g = 0$ p.u.

V. CONCLUSION

In this paper, the characteristics of a hybrid compensated transmission line with series capacitor and SSSC is analyzed. The converters are modeled using switching functions. The time invariant model is derived based on D-Q variables. The predictions about the stability of torsional modes using various methods of analysis shows good agreement. A simple technique for the extraction of subsynchronous frequency components using filters is proposed. Filter gains are optimized using GA and is based on damping torque analysis.

The following points emerge based on the results of the case study.

1) The SSSC is not strictly SSR neutral, however it offers a reactance which remains practically constant with frequency and increases the electrical resonant frequency of the network when constant reactive voltage control is adopted.

2) The inclusion of SSSC reduces the risk of SSR by detuning the network resonant frequency. Although the introduction of SSSC reduces the peak negative damping, properly designed subsynchronous current suppressor improves the damping of all the critical torsional modes.

3) The subsynchronous current suppressor effectively improves the damping of torsional modes in the entire range of compensation level and for the different operating conditions.

4) The SSCS is effective in extracting and suppressing the subsynchronous frequency components of line current under various disturbances even when the operating point fundamental frequency line current is zero.

5) The risk of SSR is totally eliminated with the inclusion of subsynchronous current suppressor as electrical resonance condition is eliminated in the practical range of series compensation levels.

REFERENCES

[1] M. C. Hall and D. A. Hodges, "Experience with 500 kV subsynchronous resonance and resulting turbine generator shaft damage at Mohave generating station," in *Analysis and Control of Subsynchronous Resonance*, 1976, IEEE Publ. 76 CH 1066-O-PWR.

[2] C. E. J. Bowler, D. N. Ewart, and C. Concordia, "Self excited torsional frequency oscillations with series capacitors," *IEEE Trans. Power App. Syst.*, vol. PAS-92, pp. 1688–1695, 1973.

[3] L. A. Kilgore, D. G. Ramey, and M. C. Hall, "Simplified transmission and generation system analysis procedures for subsynchronous resonance problems," *IEEE Trans. Power App. Syst.*, vol. PAS-96, pp. 1840–1846, Nov./Dec. 1977.

[4] K. R. Padiyar, *Analysis of Subsynchronous Resonance in Power Systems*. Boston, MA: Kluwer, 1999.

[5] K. R. Padiyar and N. Prabhu, "Analysis of subsynchronous resonance with three level twelve-pulse VSC based SSSC," in *Proc. IEEE TENCON-2003*, Oct. 14–17, 2003.

[6] K. R. Padiyar and N. Prabhu, "A comparative study of SSR characteristics of TCSC and SSSC," in *Proc. PSCC Conf. 2005*, Liege, Belgium, Aug. 2005.

[7] M. Bongiorno, J. Svensson, and L. Angquist, "Online estimation of subsynchronous voltage components in power systems," *IEEE Trans. Power Del.*, vol. 23, no. 1, pp. 410–418, Jan. 2008.

[8] M. Bongiorno, J. Svensson, and L. Angquist, "On control of static synchronous series compensator for SSR mitigation," *IEEE Trans. Power Electron.*, vol. 23, no. 2, pp. 735–743, Mar. 2008.

[9] M. Bongiorno, J. Svensson, and L. Angquist, "Single-phase VSC based SSSC for subsynchronous resonance damping," *IEEE Trans. Power Del.*, vol. 23, no. 3, pp. 1544–1552, Jul. 2008.

[10] N. G. Hingorani and L. Gyugyi, *Understanding FACTS*. New York: IEEE Press, 2000.

[11] Schauder and Mehta, "Vector analysis and control of advanced static VAR compensators," *IEE Proc.-c*, vol. 140, no. 4, pp. 299–306, Jul. 1993.

[12] K. K. Sen and E. J. Stacy, "UPFC-unified power flow controller: Theory, modelling and applications," *IEEE Trans. Power Del.*, vol. 13, no. 4, pp. 1453–1460, Oct. 1998.

[13] K. R. Padiyar, *FACTS Controllers in Power Transmission and Distribution*. New Delhi, India: New Age International, 2007.

[14] K. R. Padiyar and N. Prabhu, "Design and performance evaluation of subsynchronous damping controller with STATCOM," *IEEE Trans. Power Del.*, vol. 21, no. 3, pp. 1398–1405, Jul. 2006.

[15] K. R. Padiyar, *Power System Dynamics—Stability and Control*, 2nd ed. Hyderabad, India: B.S. Publications, 2002.

[16] "First bench mark model for computer simulation of subsynchronous resonance," *IEEE Trans. Power App. Syst.*, vol. PAS-96, no. 5, pp. 1565–1572, Sep./Oct. 1977.

[17] *Using MATLAB-SIMULINK*. Natick, MA: MathWorks, 1999.

[18] N. Prabhu and K. R. Padiyar, "Investigation of subsynchronous resonance with VSC based HVDC transmission systems," *IEEE Trans. Power Del.*, vol. 24, no. 1, pp. 433–440, Jan. 2009.

[19] K. R. Padiyar and V. Swayam Prakash, "Tuning and performance evaluation of damping controller for a STATCOM," *Int. J. Elect. Power Energy Syst.*, vol. 25, pp. 155–166, 2003.

[20] Goldberg, *Genetic Algorithm in Search, Optimization and Machine Learning*. Reading, MA: Addison Wesley, 1989.

R. Thirumalaivasan (M'12) received the B.E. degree from Madras University, Chennai, India, in 1999 and the M.Tech degree from the College of Engineering, Anna University, Guindy, Chennai, in 2002. He is pursuing the Ph.D. degree in the Department of Electrical Engineering, JNTU Hyderabad, India.

He is an Assistant Professor (Senior) in the School of Electrical Engineering at VIT University, Vellore, India. His research interests include FACTS, HVDC, and real-time digital simulation of power electronics and power systems.

M. Janaki (M'12) received the B.E. degree from Madras University, Chennai, India, in 1996 and the M.E degree from the College of Engineering, Anna University, Guindy, Chennai, in 2002. She is pursuing the Ph.D. degree in the Department of Electrical Engineering, JNTU Hyderabad, India.

She is an Assistant Professor (Senior) in the School of Electrical Engineering at VIT University, Vellore, India. Her research interests include FACTS, HVDC, and power systems.

Nagesh Prabhu (M'08) received the Dipl. Elect. Engg. degree from Karnataka Polytechnic, Mangalore, India, in 1986. He graduated in Electrical Engineering from the Institution of Engineers (India) in 1991, received the M.Tech. degree in power and energy systems from N.I.T. Karnataka, India (formerly Karnataka Regional Engineering College) in 1995, and the Ph.D. degree from the Indian Institute of Science, Bangalore, India, in 2005.

He is presently Principal, Canara Engineering College, Mangalore, India. He was with N.M.A.M Institute of Technology, Nitte, India, from 1986 to 1998, served in J.N.N. College of Engineering Shimoga, India, from 1998–2006 and at the Vel Multi Tech Sri Rangarajan Sakunthala Engineering College from 2006–2008 prior to joining CEC Mangalore. His research interests are in the area of power system dynamics and control, HVDC and FACTS, and custom power controllers.

Dr. Prabhu is a life member of the Indian Society for Technical Education and a Fellow of ISLE, India.